Available online at www.sciencedirect.com

ScienceDirect

Procedia IUTAM 15 (2015) 172 – 177

Procedia IUTAM

www.elsevier.com/locate/procedia

IUTAM Symposium on Multiphase flows with phase change: challenges and opportunities, Hyderabad, India (December 08 – December 11, 2014)

Electrostatic suppression of the "coffee-stain effect"

Alexander W. Wray[a], Demetrios T. Papageorgiou[b], Richard V. Craster[b], Khellil Sefiane[c], Omar K. Matar[a]

[a]*Department of Chemical Engineering, Imperial College London, South Kensington Campus, SW7 2AZ, UK*
[b]*Department of Mathematics, Imperial College London, South Kensington Campus, SW7 2BZ, UK*
[c]*Institute for Materials and Processes, School of Engineering, The University of Edinburgh, King's Buildings, Mayfield Road, Edinburgh EH9 3JL, UK*

Abstract

The dynamics of a slender, nano-particle laden droplet are examined when it is subjected to an electric field. Under a long-wave assumption, the governing equations are reduced to a coupled pair of nonlinear evolution equations prescribing the dynamics of the interface and the depth-averaged particle concentration. This incorporates the effects of viscous stress, capillarity, electrostatically-induced Maxwell stress, van der Waals forces, evaporation and concentration-dependent rheology. It has previously been shown [27] that electric fields can be used to suppress the ring effect typically exhibited when such a droplet undergoes evaporation. We demonstrate here that the use of electric fields affords many diverse ways of controlling the droplets.

Peer-review under responsibility of Indian Institute of Technology, Hyderabad.

Keywords: electrostatics, thin-film, droplet, nanoparticles, evaporation

1. Introduction

The commonly experienced 'ring-stain' effect - the characteristic residue left behind by an evaporating coffee droplet - has received significant attention in recent times both theoretically and experimentally [1,6,7,13,14,20,22,10,25,15,11,8,23,5]. This is thanks in part to its influence and impact on a wide array of industrial applications such as nanofabrication [16,19], sample manipulation [2,12,18] and self-assembly [24], as well as many others [3,28]. It has recently been shown that electric fields can have a pronounced effect on the formation (or lack thereof) of these rings [9,21]. However, thus far theoretical considerations have been confined to attempts to suppress this ring-stain effect [27]; it is clear that many other opportunities are afforded by these electric fields, and indeed that these opportunities are industrially relevant. We will therefore exploit this existing model to investigate the degree of the control.

E-mail address: aw1109@imperial.ac.uk

Peer-review under responsibility of Indian Institute of Technology, Hyderabad.
doi:10.1016/j.piutam.2015.04.024

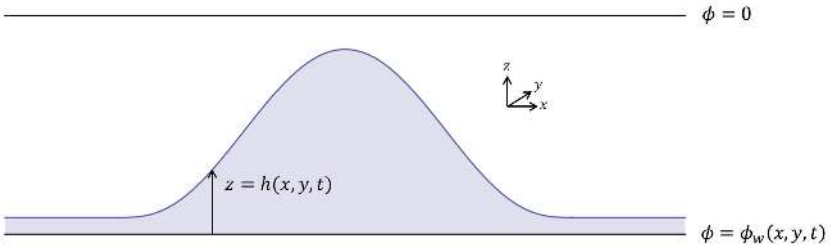

Fig. 1. Schematic of scenario being considered. Upper surface is a grounded electrode; the potential of the bottom electrode is given as $\phi_w(x, t)$.

In Section 2 we formulate the problem and produce a low-order model via the use of long-wave asymptotics. In Section 3 we demonstrate a variety of possible manipulations of these droplets. Finally we give our conclusions in Section 4.

2. Problem Formulation

We consider a droplet of viscosity μ and density ρ deposited on an ultrathin precursor film, resting on top of a flat horizontal substrate. A schematic is given in Figure 1. The liquid is assumed sufficiently viscous that the hydrodynamic portion of the problem is governed by the Stokes equations, subject to no-slip at the lower wall and appropriate stress conditions at the interface,

$$\nabla p = \mu \nabla^2 \mathbf{u}, \tag{1}$$

$$\mathbf{u}|_{z=0} = 0, \tag{2}$$

$$\mathbf{n} \cdot \mathbf{T} \cdot \mathbf{n} = \Pi - \gamma \nabla_s \cdot \mathbf{n}, \quad \mathbf{n} \cdot \mathbf{T} \cdot \mathbf{t} = \mathbf{t} \cdot \nabla_s \gamma. \tag{3}$$

A second parallel surface above the droplet acts as a grounded electrode; the surface on which the droplet rests has a spatiotemporally varying potential $\phi_w(x, t)$. The liquid and gas regions repsectively are assumed to have relative permittivies ϵ_L and ϵ_G, and a conducivity ratio σ_R. It is assumed that the electrical conductivities in each region are sufficiently high that they satisfy the continuity of current at the interface, as well as equipotential there. The potentials $\phi^{L,G}$ satisfy Laplace's equation so that

$$\nabla^2 \phi^{L,G} = 0, \tag{4}$$

$$\phi^L|_{z=0} = \phi_W, \quad \phi^G|_{z=d} = 0, \quad \phi^L|_{z=h} = \phi^G|_{z=h}, \tag{5}$$

$$\sigma_R \left(\mathbf{n} \cdot \nabla \phi^L \right)\Big|_{z=h} = \left(\mathbf{n} \cdot \nabla \phi^G \right)\Big|_{z=h}, \tag{6}$$

where $z = h$ is the position of the interface. The electrostatics enter the model via an induced Maxwell stress $\mathcal{M}^e$, whose contribution to the total stress $\mathbf{T}$ is given by

$$\mathcal{M}^e = \epsilon \mathbf{E}\mathbf{E} - \frac{1}{2}\epsilon |\mathbf{E}|^2 \mathbf{I}. \tag{7}$$

We assume a diffusion-limited model for the evaporative effects[5], induced by heating the substrate above the saturation temperature. The temperature distribution T is assumed to be conduction dominated so that it satisfies Laplace's equation subject to a thermal flux condition at the interface, and a thermal equilbrium condition at the wall,

$$\nabla^2 T = 0, \quad \Delta H_v J = -\lambda \mathbf{n} \cdot \nabla\, T|_{z=h}, \quad T|_{z=0} = T_w, \tag{8}$$

where ΔH_v is the latent heat of vaporization, λ is the thermal conductivity, J is the evaporative flux, and T_w is the temperature of the wall. The system is closed by an appropriate interfacial condition and saturation temperature relation, respectively

$$\frac{p_{ve}}{p_v} - 1 = \frac{1}{\rho_l R T_s}(p - p_v) + \frac{\Delta H_v}{R T_s}\left(\frac{T_i}{T_s} - 1\right), \quad T_s = \frac{2\pi}{R}\left(\frac{J}{\rho_V\left(\frac{p_{ve}}{p_v} - 1\right)}\right)^2 \tag{9}$$

where T_i is the interfacial temperature, R is the gas constant per unit volume, p_v is the pressure of the vapor phase, p_{ve} is the equilibrium vapor pressure, T_s is the saturation temperature and ρ_v is the vapor density. The droplet is taken to contain nanoparticles of density c_ρ which are assumed to follow an advection-diffusion equation with diffusion coefficient $\mathcal{D}$, in a low-Peclet number limit, treated with the common depth-averaging method[17].

In order to make analytical progress, we exploit the fact that we are working in a long-wave regime, making appropriate non-dimensionalisations, together with the substitutions $x = \tilde{x}/\delta, \widetilde{Ca} = \delta^{-3}\mu_0 V/\gamma_0, Pe = \delta^{-1}V\mathcal{L}/\mathcal{D}, E_b = \delta\,\epsilon_0\phi_b^2/(\mu_0 V\mathcal{L}), Ma = \delta^2\sigma_0 T_s/(V\mu_0), K = (2\pi R T_s)^{1/2}\rho_l V/(\rho_V \Delta H_v), \Delta = \delta^{-2}V\mu_0/(\rho_l \Delta H_v \mathcal{L}), T = T_s\left(1+\delta\hat{T}\right)$, where δ is a slenderness parameter given by the aspect ratio of the drop. This ultimately leads to the governing equations[27],

$$h_t + \nabla\cdot\left[\frac{h^2}{2\mu}\left(Ma\nabla(Jh) + E_b\frac{\epsilon_G\phi_w}{h-d}\nabla\phi_w\right) - \frac{1}{3\mu}h^3\nabla p\right] + J = 0, \tag{10}$$

$$(hc)_t + \nabla\cdot\left[\frac{h^2 c}{2\mu}\left(Ma\nabla(Jh) + E_b\frac{\epsilon_G\phi_w}{h-d}\nabla\phi_w\right) - \frac{1}{3\mu}h^3 c\,\nabla p\right] = \frac{\nabla\cdot(h\nabla c)}{Pe}, \tag{11}$$

where $J = \frac{\Theta+\Delta p}{K+h}$. These are solved subject to the initial conditions

$$h(x,y,0) = \begin{cases}(1-r^2)^3 + h_\infty & r \le 1\\ h_\infty, & r > 1\end{cases} \tag{12}$$

$$hc(x,y,0) = 0.1 \times h(x,y,0). \tag{13}$$

where $r^2 = x^2 + y^2$.

3. Results

It has previously been seen[27] that values of $\Delta = 0.005$, $K = 0.2$ and $\Theta = 0.2$ give rise to patterns similar to those seen experimentally, and therefore these are used throughout. These variables respectively denote the relative significance of pressure variation on the phase-change interfacial temperature, of interfacial kinetic effects, and the superheat. We use carefully chosen electric fields to demonstrate a variety of control mechanisms. In order to allow the droplets to settle from their articifial initial condition, we allow

$$E_b = \mathcal{E}(1 - \exp(-10t)). \tag{14}$$

The resultant equations represent a stiff, highly coupled system requiring a fine spatial resolution. In order to solve these accurately and quicky, we use a semi-implicit scheme based on the pseudolinear scheme (pL_1) of Witelski & Bowen[26].

3.1. Drop splitting

We first demonstrate the ability to cut droplets into multiple pieces. Based on previous results[27,4], we know that the fluid will have a tendency to flow away from areas of lower potential towards areas of higher potential. Therefore, we start by cutting the droplet into two pieces using the field

$$\phi_w(x,y) = 1 - \exp(-10x^2), \quad \mathcal{E} = 300, \quad d = 2.5. \tag{15}$$

The resultant evolution is given in Figure 2. It is readily seen that the droplet is divided into two pieces by the field.

This principle can be arbitrarily extended to cut droplets in more intricate ways. For example, the field

$$\phi_w(x,y) = 2 - \exp(-10x^2) - \exp(-10y^2), \quad \mathcal{E} = 300, \quad d = 2.5 \tag{16}$$

gives rise to the division of droplets shown in Figure 3.

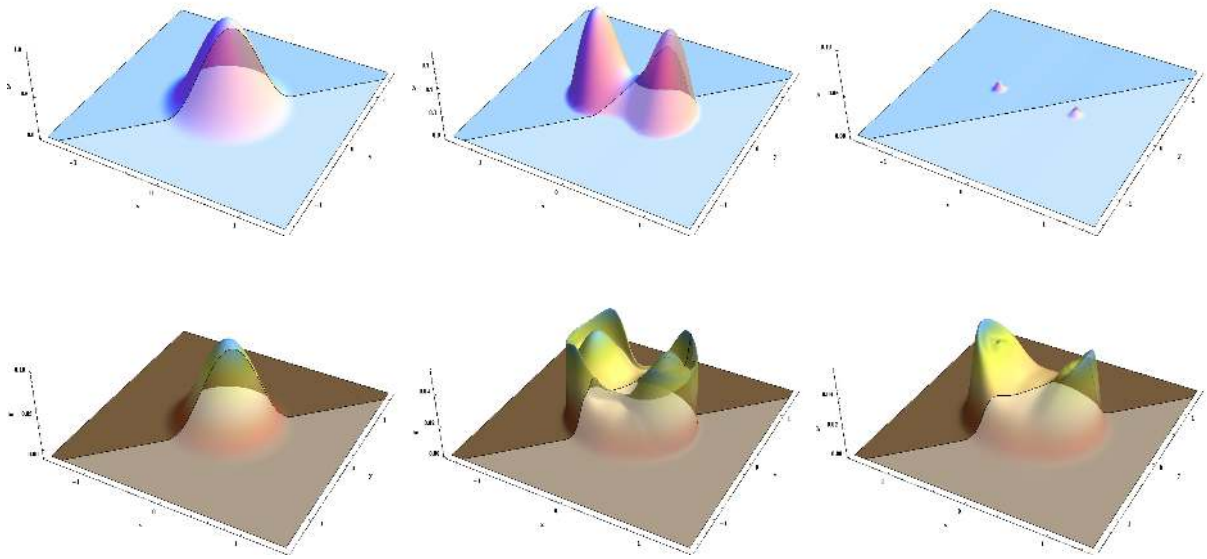

Fig. 2. Results of the two-dimensional calculations for the field (15). The upper row gives the interfacial position h while the lower row gives the particle distribution hc. Left: $t = 0$; middle: $t = 0.6$; right: $t = 1.2$. The drop initially divides into two daughter droplets. During their subsequent evaporation, this gives rise to two independent structures for the particles; one from each daughter droplet. At higher values of Θ and lower values of K these structures are known to become successively more ring-like.[27]

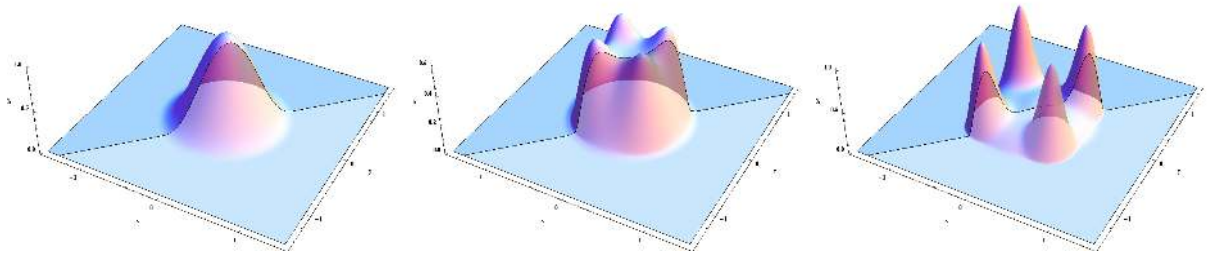

Fig. 3. Results of calculations for the field (16); interfacial position h is given. Left: $t = 0$; middle: $t = 0.5$; right: $t = 1$. The drop is divided into four smaller drops.

3.2. Drop movement

We demonstrate an example of moving a droplet. From hereon, we ignore evaporative effects. We use the linear potential

$$\phi_w = \frac{L_y}{2} + y, \quad \mathcal{E} = 100, \quad d = 10, \tag{17}$$

where L_y is the length of the domain in the y-direction. This gives a field that will drive fluid towards positive y. We see the results in Figure 4. As expected the droplet is moved along the domain.

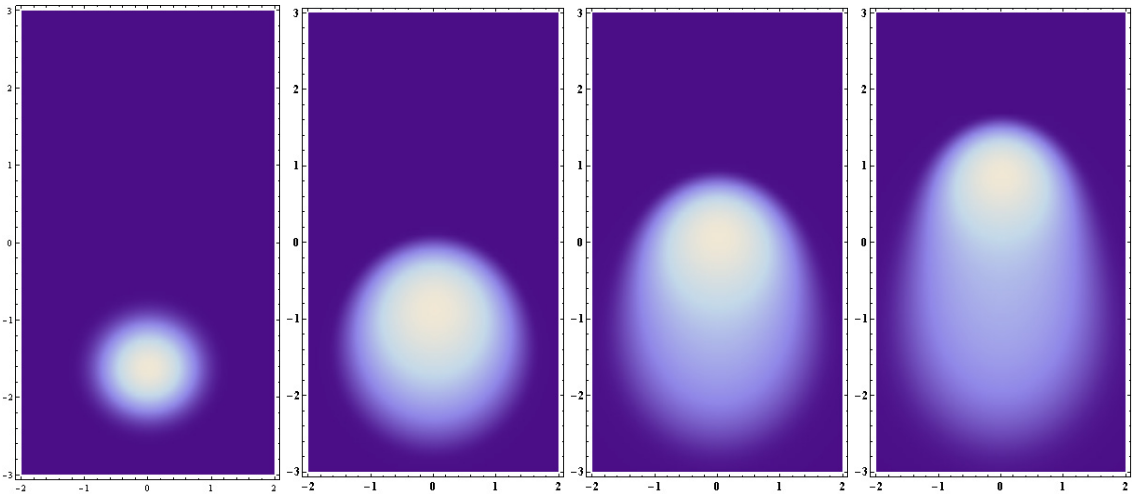

Fig. 4. Results of the two-dimensional calculations for the field (17). Left to right: $t = 0$, $t = 10$, $t = 30$ and $t = 50$. The drop moves up across the domain.

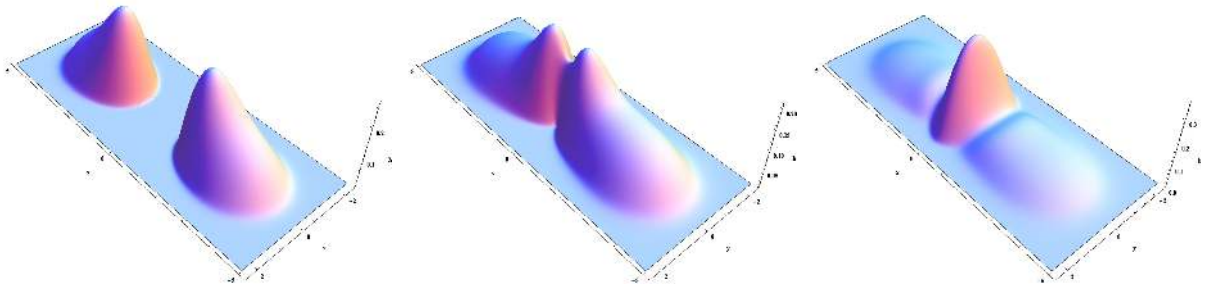

Fig. 5. Results of the two-dimensional calculations for the field (18). Left: $t = 25$; middle: $t = 54$; right: $t = 100$. The drops move towards one another and subsequently coalesce rapidly. Note that the final state is not a circular droplet, due to the continued presence of the electric field.

3.3. Drop coalescence

Given the ability to move drops arbitrarily, we can of course arrange for coalescence. We therefore change our initial condition to have droplets centred at $(-3.4, 0)$ and $(3.4, 0)$. We then impose the electric field

$$\phi_w(x, y) = \frac{L_x}{2} - |x|\,, \quad \mathcal{E} = 100, \quad d = 10 \tag{18}$$

where L_x is the length of the domain in the x-direction (in this case $L_x = 10$). As we see in Figure 5, the effect of the electric field is to push the two droplets towards each other until they touch, and then the two begin to coalesce rapidly.

4. Conclusions

The three-dimensional behaviour of a nanoparticle-laden droplet has been considered under manipulation by electric fields.

A long-wave approximation has been applied to derive a low-order model prescribing the behaviour of the droplet, incorporating the effects of concentration-dependent viscosity, capillarity, Marangoni stress and Maxwell stress. The resultant equations have been solved using an operator-splitting technique.

Via the use of appropriately chosen electric potentials, we have shown that droplets can be divided up or moved around, allowing for delicate active control scenarios, including potentially inducing coalescence.

References

1. Eiki Adachi, Antony S Dimitrov, and Kuniaki Nagayama. Stripe patterns formed on a glass surface during droplet evaporation. *Langmuir*, 11(4):1057–1060, 1995.
2. Ralf Blossey and Andreas Bosio. Contact line deposits on cdna microarrays: a "twin-spot effect". *Langmuir*, 18(7):2952–2954, 2002.
3. Hugues Bodiguel, Frédéric Doumenc, and Béatrice Guerrier. Stick- slip patterning at low capillary numbers for an evaporating colloidal suspension. *Langmuir*, 26(13):10758–10763, 2010.
4. R V Craster and O K Matar. Electrically induced pattern formation in thin leaky dielectric films. *Phys. Fluids*, 17:032104, 2005.
5. R V Craster, O K Matar, and Khellil Sefiane. Pinning, retraction, and terracing of evaporating droplets containing nanoparticles. *Langmuir*, 25(6):3601–3609, 2009.
6. Robert D Deegan, Olgica Bakajin, Todd F Dupont, Greb Huber, Sidney R Nagel, and Thomas A Witten. Capillary flow as the cause of ring stains from dried liquid drops. *Nature*, 389(6653):827–829, 1997.
7. Robert D Deegan, Olgica Bakajin, Todd F Dupont, Greg Huber, Sidney R Nagel, and Thomas A Witten. Contact line deposits in an evaporating drop. *Phys. Rev. E: Stat., Nonlinear, Soft Matter Phys.*, 62(1):756–765, 2000.
8. GJ Dunn, SK Wilson, BR Duffy, S David, and K Sefiane. The strong influence of substrate conductivity on droplet evaporation. *J. Fluid Mech.*, 623:329–351, 2009.
9. H Burak Eral, D Mampallil Augustine, MHG Duits, and Frieder Mugele. Suppressing the coffee stain effect: how to control colloidal self-assembly in evaporating drops using electrowetting. *Soft Matter*, 7(10):4954–4958, 2011.
10. Benjamin J Fischer. Particle convection in an evaporating colloidal droplet. *Langmuir*, 18(1):60–67, 2002.
11. Fabien Girard, Mickaël Antoni, Sylvain Faure, and Annie Steinchen. Evaporation and marangoni driven convection in small heated water droplets. *Langmuir*, 22(26):11085–11091, 2006.
12. T Heim, S Preuss, B Gerstmayer, A Bosio, and R Blossey. Deposition from a drop: morphologies of unspecifically bound dna. *J. Phys.: Condens. Matter*, 17(9):S703–S716, 2005.
13. Hua Hu and Ronald G Larson. Evaporation of a sessile droplet on a substrate. *J. Phys. Chem. B*, 106(6):1334–1344, 2002.
14. Hua Hu and Ronald G Larson. Analysis of the microfluid flow in an evaporating sessile droplet. *Langmuir*, 21(9):3963–3971, 2005.
15. Hua Hu and Ronald G Larson. Marangoni effect reverses coffee-ring depositions. *J. Phys. Chem. B*, 110(14):7090–7094, 2006.
16. Jiaxing Huang, Andrea R Tao, Stephen Connor, Rongrui He, and Peidong Yang. A general method for assembling single colloidal particle lines. *Nano Lett.*, 6(3):524–529, 2006.
17. O E Jensen and J B Grotberg. The spreading of heat or soluble surfactant along a thin liquid film. *Phys. Fluids A*, 5(1):58–68, 1993.
18. Yongseong Kim, Gregory B Hurst, Mitchel J Doktycz, and Michelle V Buchanan. Improving spot homogeneity by using polymer substrates in matrix-assisted laser desorption/ionization mass spectrometry of oligonucleotides. *Anal. Chem.*, 73(11):2617–2624, 2001.
19. Michael Layani, Michael Gruchko, Oded Milo, Isaac Balberg, Doron Azulay, and Shlomo Magdassi. Transparent conductive coatings by printing coffee ring arrays obtained at room temperature. *ACS Nano*, 3(11):3537–3542, 2009.
20. Kara L Maki and Satish Kumar. Fast evaporation of spreading droplets of colloidal suspensions. *Langmuir*, 27(18):11347–11363, 2011.
21. D Mampallil, H B Eral, D van den Ende, and F Mugele. Control of evaporating complex fluids through electrowetting. *Soft Matter*, 8(41):10614–10617, 2012.
22. Hassan Masoud and James D Felske. Analytical solution for stokes flow inside an evaporating sessile drop: Spherical and cylindrical cap shapes. *Phys. Fluids*, 21:042102, 2009.
23. O K Matar, R V Craster, and K Sefiane. Dynamic spreading of droplets containing nanoparticles. *Phys. Rev. E: Stat., Nonlinear, Soft Matter Phys.*, 76(5):056315, 2007.
24. David J Norris, Erin G Arlinghaus, Linli Meng, Ruth Heiny, and LE Scriven. Opaline photonic crystals: How does self-assembly work? *Adv. Mater. (Weinheim, Ger.)*, 16(16):1393–1399, 2004.
25. AJ Petsi and VN Burganos. Stokes flow inside an evaporating liquid line for any contact angle. *Phys. Rev. E: Stat., Nonlinear, Soft Matter Phys.*, 78(3):036324, 2008.
26. T.P. Witelski and M. Bowen. Adi schemes for higher-order nonlinear diffusion equations. *Appl. Numer. Math.*, 45(2):331–351, 2003.
27. Alexander William Wray, Demetrios T Papageorgiou, Richard V Craster, Khellil Sefiane, and Omar Kamal Matar. Electrostatic suppression of the 'coffee-stain effect'. *Langmuir*, 2014.
28. Dongmao Zhang, Yong Xie, Melissa F Mrozek, Corasi Ortiz, V Jo Davisson, and Dor Ben-Amotz. Raman detection of proteomic analytes. *Anal. Chem.*, 75(21):5703–5709, 2003.